PNAS RESEARCH ARTICLE | NEUROSCIENCE

Neuromodulation of swarming behavior in *Caenorhabditis elegans*: Insights into the conserved role of calsyntenins

Navneet Shahi[a,1], Nisha Kumari[a,b,2], Sharveri Khapre[a], Dimple Dahiya[a,c], Egemen Saritekin[d], Aşkın Kocabaş[d], and Kavita Babu[a,1]

Affiliations are included on p. 11.

Edited by Michael O'Donnell, Yale University, New Haven, CT; received July 24, 2025; accepted January 14, 2026 by Editorial Board Member John R. Carlson

Collective animal behaviors arise from a complex interplay between internal physiological states and external environmental cues. In *Caenorhabditis elegans*, favorable conditions promote dispersal, while stressors like food scarcity trigger aggregation. Here, we describe a distinct self-organized swarming behavior, where *C. elegans* move and feed in groups driven by uncontrolled local increases in population density despite abundant food availability. While various environmental factors have been implicated in collective behaviors in *C. elegans*, the underlying genetic and molecular mechanisms remain unclear. We identify a key role for the conserved calsyntenin protein CASY-1 in regulating swarming. Through genetic, behavioral, and optogenetic approaches, we show that CASY-1 functions to modulate the neuropeptide pigment-dispersing factor (PDF) signaling. Mutants in *casy-1* show impaired PDF-1 signaling and reduced inhibition of the serotonin pathway, a known regulator of social behaviors. This dysregulation, along with its associated mechanosensory and foraging defects, likely contributes to the swarming phenotype. Our findings reveal a putative neuromodulatory pathway critical for swarming behavior in *C. elegans*.

Calsyntenin | *C. elegans* | swarming | serotonin

The ability of animals to group or disperse is rarely random. It reflects a complex integration of diverse sensory, physiological, and environmental cues (1–6). Across species, collective behaviors such as coordinated migration, social feeding, and cooperative defense have evolved as adaptive strategies, seen in ant trails, bird flocks, fish shoals, and mammalian herds (6–11). Yet, the underlying neural mechanisms that translate complex cues into coordinated group actions remain poorly understood.

The nematode *Caenorhabditis elegans* offers a powerful system to dissect the genetic and neural basis of collective behavior, owing to its well-characterized nervous system and ease of culturing large populations (12). *C. elegans* exhibits a wide repertoire of collective behaviors, including social feeding, aggregation, swarming, and towering (7, 13–15). These behaviors are strongly modulated by environmental factors such as food distribution (16, 17), pheromones (5, 18, 19), oxygen (20–22), pathogen exposure (18, 22, 23), and population density (17, 22). Among them, two distinct mechanisms are known to govern swarming: oxygen sensing in natural isolates (*npr-1*) and population density in the laboratory reference strain N2. Natural isolates, also termed "social feeders," display high oxygen sensitivity, which drives spontaneous group formation and collective swarming (20–22). In contrast, the N2 strain typically behaves solitarily but engages in large-scale swarming only at artificially elevated population densities (17, 22). In this study, we report a distinct swarming behavior that differs fundamentally from previously characterized N2 and *npr-1*-mediated mechanisms. This swarming state emerges through self-organization driven by uncontrolled local increases in population density of otherwise solitary animals, yet it does not rely on oxygen sensitivity. Our study expands the current models of *C. elegans* collective behavior and highlights the role of internal molecular and neuromodulatory regulators.

Disruptions in social behavior are a hallmark of several neurodevelopmental disorders, including autism, bipolar disorder, and schizophrenia (7, 24–26). These impairments are often associated with genes involved in sensory integration and neuromodulation (6, 7). Thus, identifying such genes can offer valuable insight into the biological mechanisms underlying social dysfunction in these disorders. In this context, we investigate the role of CASY-1, the *C. elegans* ortholog of mammalian calsyntenin proteins (27). Calsyntenins have been linked to multiple neuropsychiatric conditions marked by social deficits (28–32). Although CASY-1 has been studied in the context of synaptic

Significance

Starved yet social: Decoding why worms swarm on food instead of dispersing. We identify a distinct, self-organized collective behavior in which worms cluster at the food boundary and fail to disperse. Although this behavior hampers optimal development and leads to starvation, animals remain confined even in the presence of abundant food. We show that this spontaneous swarming is regulated by the conserved trafficking protein, CASY-1. Loss of *casy-1* disrupts the balance between opposing signals, serotonin and neuropeptide PDF-1, resulting in reduced exploration and increased local crowding. By linking molecular regulation, neural activity, and population-level dynamics, our work provides an understanding of how internal neural processes give rise to collective behavior, with broader relevance to social behavior across species.

The authors declare no competing interest.

This article is a PNAS Direct Submission. M.O. is a guest editor invited by the Editorial Board.

Copyright © 2026 the Author(s). Published by PNAS. This article is distributed under Creative Commons Attribution-NonCommercial-NoDerivatives License 4.0 (CC BY-NC-ND).

[1]To whom correspondence may be addressed. Email: navneetshahi@iisc.ac.in or kavitababu@iisc.ac.in.

[2]Present address: Department of Biology, Katholieke Universiteit Leuven, Leuven 3000, Belgium.

This article contains supporting information online at https://www.pnas.org/lookup/suppl/doi:10.1073/pnas.2520029123/-/DCSupplemental.

Published February 17, 2026.

Downloaded from https://www.pnas.org by KOC UNIVERSITY LIBRARY on August 11, 2026 from IP address 88.255.99.16.

transmission (33–35), chemotaxis (27), and memory formation (36, 37), its mechanisms in regulating social interactions are not well understood.

Classically, the neuropeptide receptor NPR-1 has been extensively studied for its role in diverse collective behaviors in *C. elegans* (20, 38, 39). In parallel, a broader set of conserved neuromodulators contributes to the regulation of social behavioral states. Serotonin, in particular, is a highly conserved regulator of social behavior across species, modulating group aggregation in locusts (3), and shaping context-dependent social responses in crustaceans, fish, rodents, and primates (40–42). Dysregulation of serotonergic signaling is associated with neuropsychiatric conditions characterized by altered social behavior, including autism spectrum disorders and social anxiety (43–45). In *C. elegans*, serotonin and the neuropeptide Pigment Dispersing Factor-1 (PDF-1) function antagonistically, with serotonin inhibiting PDF-1 signaling (46, 47). PDF-1, in turn, regulates arousal (48, 49), mating interactions (50), and foraging behavior (49, 51, 52), positioning these pathways as key modulators of behavioral state transitions.

Here, we report a previously uncharacterized regulatory mechanism through which CASY-1 constrains swarming behavior. Mutants in *casy-1* form aggregates at the edge of a bacterial food lawn and fail to disperse, despite abundant food availability. These animals experience starvation and delayed development but continue to cluster, exhibiting a phenotype that resembles compulsive group-seeking behavior (53). We identify CASY-1 as a critical upstream regulator of the serotonergic–PDF-1 neuromodulatory axis. Using genetic, behavioral, and optogenetic approaches, we find that loss of *casy-1* reduces PDF-1 signaling, resulting in disinhibition of serotonin pathways. This shift modulates the activity of downstream AIY neurons, resulting in the emergence of swarming phenotype. These findings place CASY-1 as a molecular node that maintains balance between antagonistic neuromodulatory systems and reveal how disruptions to this balance can reorganize population-level behavior.

Results

CASY-1 Regulates Swarming via Its C-Terminal Domain in Sensory and Interneurons. Our interest into CASY-1's role in collective behavior began with a serendipitous observation where null mutants of *casy-1* exhibited robust self-organized swarm formations. This phenotype emerged spontaneously and reproducibly, prompting us to investigate further.

To quantify swarming, synchronized *C. elegans* were placed at one edge of a uniform bacterial lawn and recorded over 10 to 12 h. Time-lapse imaging at five equidistant time points revealed that while wild-type (WT) animals dispersed evenly across the lawn, *casy-1(ind107)* mutants formed stable aggregates at the food boundary (Movies S1 and S2). Expression of CASY-1A under its endogenous promoter significantly restored dispersal, although some variability was seen due to mosaic expression from extrachromosomal arrays (Fig. 1*A* and Movie S3).

Occasional WT aggregation was seen at early or late time points (frames 1-2 or 4-5), typically due to edge entry or food depletion, but this was transient and less prominent than *casy-1* mutants. The assay midpoint was selected for consistent quantification across replicates. Swarming was analyzed using a grayscale-based method, where higher values indicate more dispersal (Fig. 1*B*). Mid-point values were compared across genotypes (Fig. 1*C*).

The *casy-1* gene encodes three isoforms through alternative promoter usage (Fig. 1*D*). The full-length CASY-1A, containing all conserved domains, is expressed predominantly in sensory and interneurons. Shorter isoforms CASY-1B and CASY-1C lack the N-terminal region and are expressed in ventral cord motor neurons (27, 34). To determine whether CASY-1 regulates swarming through its function in sensory or motor neurons, we performed isoform-specific rescue experiments using the *Pcasy-1a* and *Pcasy-1b* promoters. Due to sequence similarity and overlapping expression, *Pcasy-1b* and *Pcasy-1c* are often used interchangeably (34).

Expression of either CASY-1A or CASY-1B under *Pcasy-1a* significantly rescued the swarming phenotype. In contrast, motor neuron–restricted expression under *Pcasy-1b* failed to do so (Fig. 1*C*). This suggests that CASY-1 acts in sensory/interneurons and that the C-terminal region alone is sufficient for rescuing the *casy-1* mutant phenotype. The *casy-1* gene encodes three isoforms through alternative promoter usage (Fig. 1*D*). The full-length CASY-1A, containing all conserved domains, is expressed predominantly in sensory and interneurons. Shorter isoforms CASY-1B and CASY-1C lack the N-terminal region and are expressed in ventral cord motor neurons (27, 34).

To test this directly, we generated CRISPR-based *casy-1* full and domain deletions (*SI Appendix*, Fig. S1 *A* and *B*). Deletion of the C-terminal domain (*ΔC*) fully phenocopied the *casy-1* null mutants. In contrast, deletion of the N-terminal domain (*ΔN*) had little or no effect (Fig. 1 *E* and *F*). These findings establish that the C-terminal domain is necessary and sufficient for regulating swarming, likely via sensory neurons.

One experimental consideration while maintaining *casy-1* mutants is their tendency to remain aggregated and failure to disperse, which complicates synchronization and uniform growth. Despite bleaching, these mutants often develop asynchronously, likely due to uneven food access and starvation. To minimize this, we plated fewer eggs at opposite ends of larger 90 mm NGM plates to improve dispersal during early development. Although slight variation in developmental stage persisted, population size was carefully calibrated across replicates to minimize variability.

To validate the robustness of the phenotype, we compared the CRISPR knockout line *casy-1(ind107)* that we had generated with two previously reported alleles, *tm718* and *wp78* (Illustrated in *SI Appendix*, Fig. S1*C*). All three alleles exhibited comparable swarming behaviors (*SI Appendix*, Fig. S1*D*). *SI Appendix*, Fig. S1*A* shows the genomic deletion in the *casy-1(ind107)* line and its genotyping. We also reproduced previously reported Aldicarb and PTZ sensitivity phenotypes associated with the *tm718* mutant line (34, 55) in the *casy-1(ind107)* animals (*SI Appendix*, Fig. S1 *E* and *F*). All subsequent experiments were performed with the *casy-1(ind107)* allele.

Swarming in *casy-1* Mutants Is Self-Organized and Independent of Known Extrinsic Sensory and Chemical Cues. To identify the sensory cues contributing to swarming in *casy-1* mutants, we examined the neuropeptide receptor NPR-1, which is a known regulator of aggregation, social feeding, and swarming (14, 17, 38, 39, 56). In *npr-1* mutants, these phenotypes are partly driven by altered oxygen sensing (20–22). Our previous work showed that *casy-1* and *npr-1* interact genetically in regulating synaptic signaling (35), prompting us to explore whether *casy-1* and *npr-1* influence swarming through similar mechanisms.

First, we compared aggregation patterns across genotypes. As expected, *npr-1* mutants formed multiple robust clusters along the food border. In contrast, *casy-1* animals remained relatively dispersed, resembling WT animals (Fig. 2*A*). This suggests that classical aggregation in *npr-1* mutants is not necessary for swarm formation in *casy-1* mutants. Next, we compared swarming behavior. Unlike *npr-1* mutants, which formed dispersed, oxygen-dependent swarms emerging from food-depleted zones, *casy-1* mutants formed

Downloaded from https://www.pnas.org by KOC UNIVERSITY LIBRARY on August 11, 2026 from IP address 88.255.99.16.

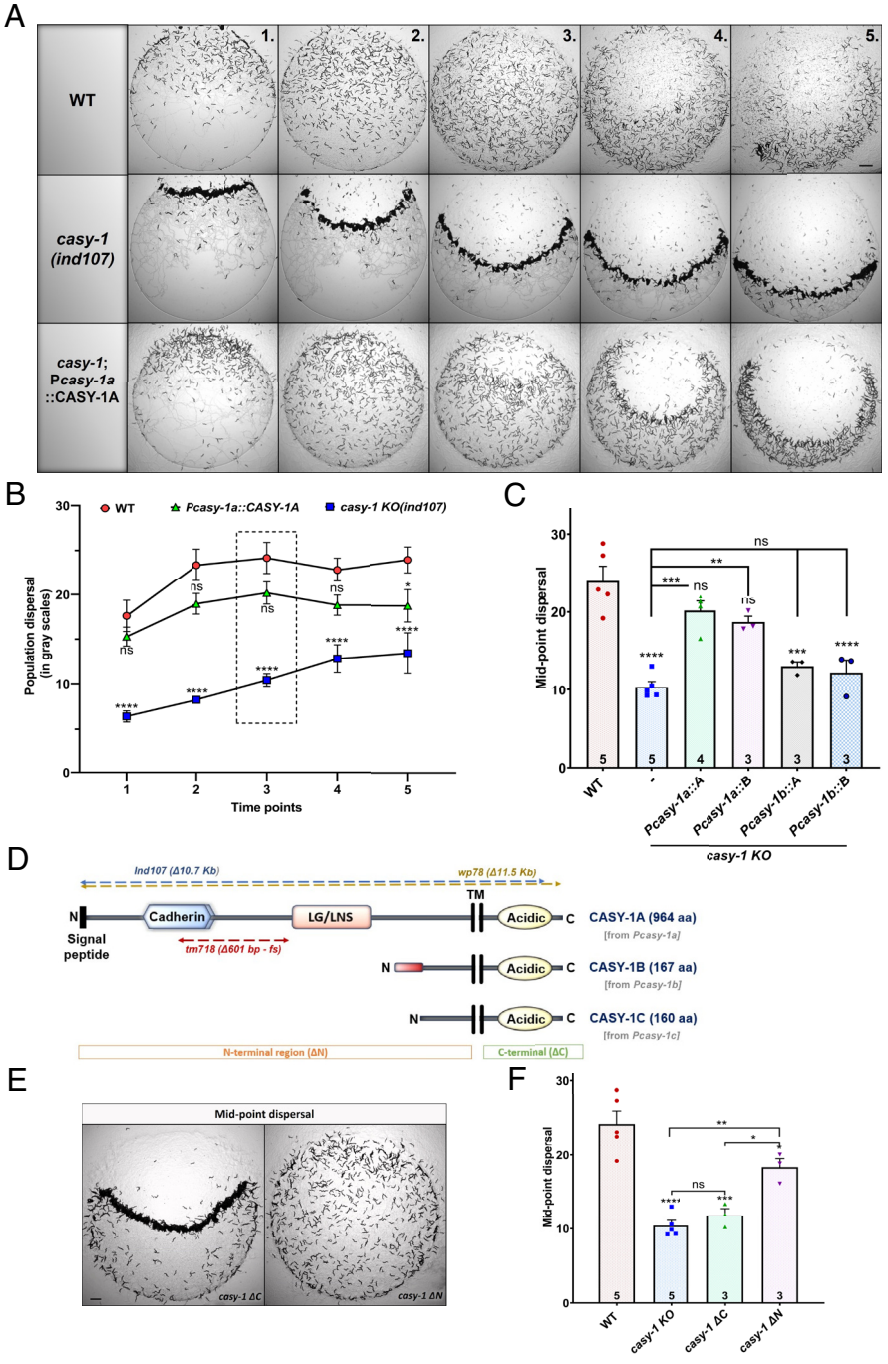

Fig. 1. CASY-1 regulates swarming via its C-terminal domain. (*A*) Time-course images showing the dispersal dynamics of wild-type (WT), *casy-1* knockout (KO), and endogenous rescue (*Pcasy-1a*::CASY-1A) *C. elegans* across a bacterial lawn at five equidistant time points. (*B*) Quantification of population dispersal using grayscale intensity across time. Lower grayscale values indicate increased clustering (swarming) and higher values indicate more dispersal. (*C*) Mid-point grayscale values used for comparison in *casy-1* mutants and isoform-specific rescue lines. Expression of CASY-1A or CASY-1B under the *Pcasy-1a* promoter significantly rescues the swarming phenotype, whereas their expression under *Pcasy-1b* does not. (*D*) Schematic of the *casy-1* locus showing three isoforms: CASY-1A (full-length, 984 aa) under *Pcasy-1a* promoter, CASY-1B (167 aa) under *Pcasy-1b*, and CASY-1C (160 aa) under *Pcasy-1c*. Isoforms B and C originate from alternative promoters within the eighth intron (~4,000 bp) of the *casy-1a* locus. Transmembrane domain (TM) demarcates the N-terminal (*casy-1 ΔN)* and C-terminal (*casy-1 ΔC)* regions. (*E*) Mid-point dispersal images of *casy-1* ΔC and *casy-1* ΔN deletions. (*F*) Quantification of dispersal in WT, *casy-1 KO*, and domain-deleted mutants. Data represent mean ± SE mean (SEM). N = 3 to 5 biological replicates, indicated inside the bar graph. Statistical significance was assessed using ordinary one-way ANOVA and Tukey's multiple comparison test. (****P* < 0.001, *****P* < 0.0001; ns = nonsignificant). (Scale bar, 1 mm.) Representative videos corresponding to this figure are available in the OSF repository (54).

compact, localized swarms. Interestingly, *casy-1; npr-1* double mutants displayed a composite phenotype, characterized by the formation of swarm-like clusters similar to *casy-1* mutants, along with enhanced peripheral dispersal seen in *npr-1* mutants (Fig. 2*B*). Although the overall dispersal area was comparable among *casy-1, npr-1,* and double mutants, their spatial organization and dynamic distribution on the food lawn differed markedly (Fig. 2 *B* and *C*), suggesting that *casy-1* and *npr-1* regulate distinct facets of swarming behavior.

To assess whether locomotory speed might explain these differences, we measured individual *C. elegans* velocities. We observed that *casy-1* mutants moved more slowly than WT animals in both on-food and off-food conditions, whereas *npr-1* mutants exhibited significantly higher speeds than WT [(14) and (*SI Appendix*, Fig. S2*A*)]. As expected from their broader dispersal, *npr-1* mutants also showed increased speed when compared to *casy-1* (*SI Appendix*, Fig. S2*A*). However, *C. elegans* speed alone could not fully explain the behavior as *casy-1; npr-1* double mutants despite having WT-like speed still exhibited swarm formation (Fig. 2*C*). It is worth noting that these are single animal speed measurements and may not indicate how speed changes in a swarm. We next asked whether *casy-1* mutants display altered oxygen sensitivity, as seen in *npr-1* (20, 22). Unlike *npr-1* mutants, *casy-1* animals responded similarly to WT across varying oxygen concentrations (*SI Appendix*, Fig. S2*B*), ruling out hypoxia-driven clustering. Swarming in WT animals typically occurs only at high population densities (22), while *npr-1* mutants can form small swarms by sensing local oxygen depletion. *casy-1* mutants also show density-dependent clustering, but their swarming arises through a mechanism independent of oxygen sensing.

Downloaded from https://www.pnas.org by KOC UNIVERSITY LIBRARY on August 11, 2026 from IP address 88.255.99.16.

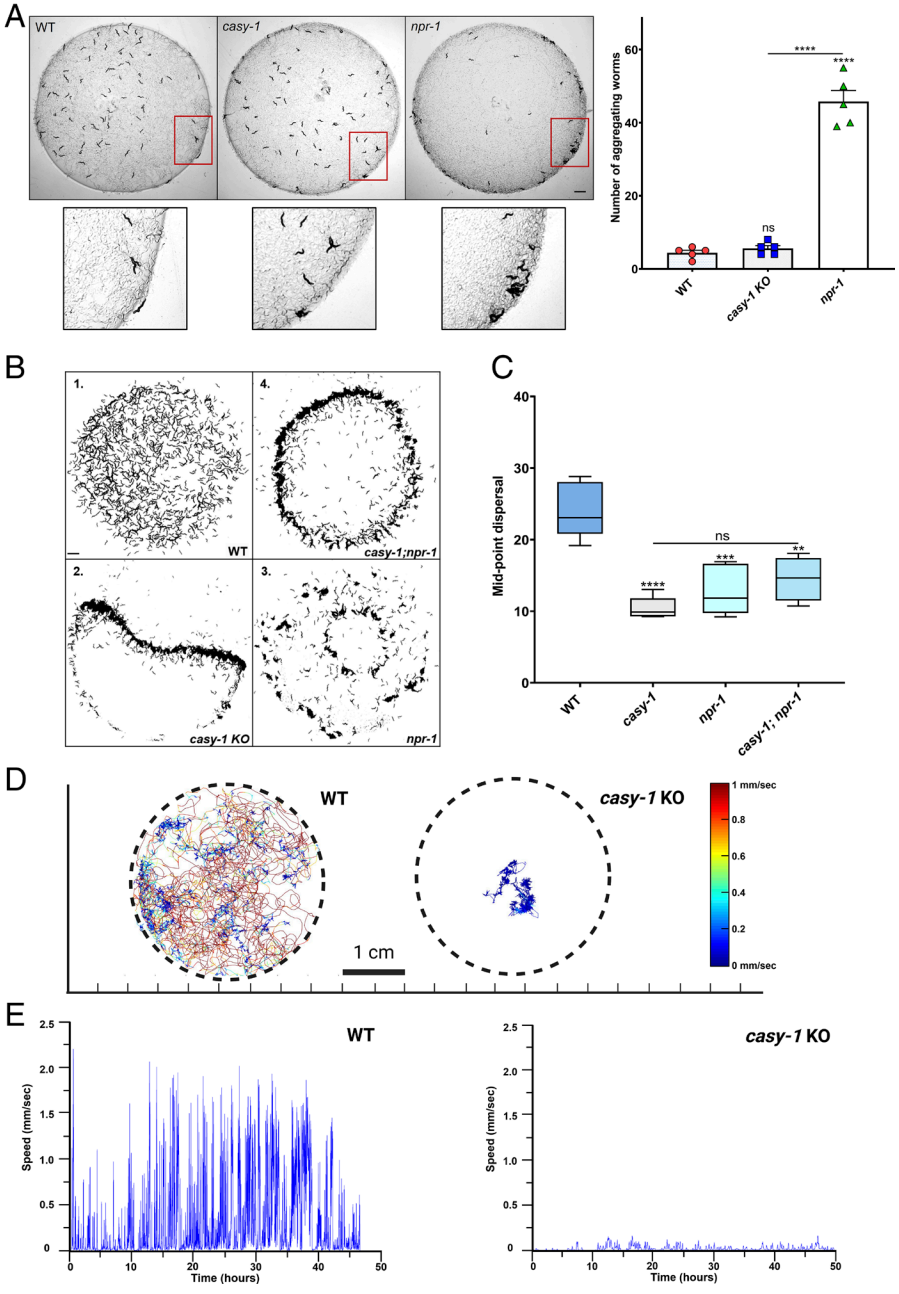

Fig. 2. *casy-1* mutants display a self-organized swarming phenotype distinct from *npr-1* mutants. (*A*) Representative images showing aggregation patterns in WT, *casy-1*, and *npr-1* mutants on a food lawn. Zoomed insets highlight *C. elegans* clustering at the food border. Quantification of the number of aggregated *C. elegans* indicates that *casy-1* mutants resemble WT and do not exhibit the border aggregation phenotype characteristic of *npr-1* mutants. (*B*) Representative images are the gray-scale snapshots of the swarming assay at the mid-point showing distinct dispersal patterns in 1. WT, 2. *casy-1*, 3. *npr-1*, and 4. *casy-1; npr-1* double mutants. Image background is removed for clear comparison of the pattern formation. (*C*) Quantification of mid-point dispersal across genotypes based on grayscale intensity measurements. The box-and-whisker plot displays the median and data range. While *casy-1* and *npr-1* mutants exhibit reduced dispersal compared to WT, no significant difference is observed between these single and double mutants. (*D*) Single-worm trajectory plots for representative WT and *casy-1* animals tracked continuously over 3 d. Each colored trace represents the movement path of an individual *C. elegans* over time, with color indicating instantaneous speed (scale shown at right). WT animals exhibit broad spatial exploration across the lawn, whereas *casy-1* mutants display highly restricted movement confined to a localized region, indicative of reduced exploration. (*E*) Corresponding speed profiles for the single-worm trajectories shown in (*D*). Plots show instantaneous speed as a function of time over the entire recording period. WT animals display frequent bouts of forward locomotion and higher speed variability, whereas *casy-1* mutants exhibit persistently low speeds with limited transitions to higher locomotor states. Data represent mean ± SEM. Biological replicates are indicated within each bar. Statistical analysis was performed using one-way ANOVA followed by Tukey's multiple comparison test (**P* < 0.05, ***P* < 0.01, ****P* < 0.001, *****P* < 0.0001; ns = nonsignificant). (Scale bar, 1 mm.) Representative videos corresponding to this figure are available in the OSF repository (54).

When *C. elegans* encounter one another in close proximity, they can engage in short-range communication that modulates social behaviors, including feeding in aggregates. Two key mediators of such interanimal signaling are pheromones and extracellular vesicles (EVs), both of which have been implicated in regulating social interactions (15, 18). To test whether these cues contribute to the swarm formation in *casy-1* mutants, we examined *daf-22* and *klp-6* mutants. *daf-22* is required for the biosynthesis of ascaroside pheromones (15, 18), while *klp-6* is involved in EV release from sensory neurons (57). Both single mutants exhibited WT-like dispersal, and the *daf-22 casy-1* and *klp-6; casy-1* double mutants continued to swarm like *casy-1* alone (*SI Appendix*, Fig. S2*C*). These results rule out a role for pheromone or EV-based communication in driving swarming in *casy-1* mutants. Further, we asked whether defective food sensation contributes to the phenotype. *odr-3* mutants, which are impaired in olfactory food detection, dispersed like WT (*SI Appendix*, Fig. S2*D*). This suggests that food sensation does not readily explain the swarming seen in *casy-1* mutants.

After ruling out a number of known extrinsic sensory and chemical cues, we asked whether swarming in *casy-1* mutants could arise from intrinsic, single-worm–level dynamics. To test this, we tracked the trajectories of ten individual young adult *C. elegans* over a period of 3 d and examined their spatial exploration and locomotion patterns. WT animals exhibited broadly distributed trajectories, repeatedly traversing the arena and covering a large area over time (Fig. 2*D* and Movie S4). In contrast, *casy-1* mutants showed highly restricted movement, remaining confined to a limited spatial region with minimal exploration. This difference was further reflected in their speed profiles, where WT *C. elegans* displayed frequent bouts of forward locomotion, whereas *casy-1* mutants exhibited persistently low speeds with rare transitions to high-velocity movement (Fig. 2*E*). Such spatial confinement and reduced locomotor dynamics are likely to promote local accumulation of animals, increasing the probability of repeated encounters and self-organized swarming.

Taken together, our findings indicate that the swarming behavior in *casy-1* mutants is not caused by altered oxygen sensing, food

Downloaded from https://www.pnas.org by KOC UNIVERSITY LIBRARY on August 11, 2026 from IP address 88.255.99.16.

sensation, pheromone signaling, or EV-mediated cues. Instead, it is more likely driven by changes in intrinsic pathways and the regulation of locomotor states.

Elevated Serotonin Signaling Underlies Swarming Behavior in *casy-1* Mutants. Given that swarming in *casy-1* mutants is self-organized and largely unaffected by extrinsic cues, we asked whether intrinsic neuromodulatory pathways contribute to this phenotype. Prior work has linked CASY-1's C-terminal domain to the vesicular trafficking and release of neuromodulators (34, 35, 58). We therefore assessed whether neurotransmitter imbalance underlies this behavior.

To address this, we screened a panel of neurotransmitter-deficient mutants affecting glutamate, GABA, acetylcholine, dopamine, octopamine, and serotonin pathways. While mutants in GABA and octopamine signaling exhibited partial swarm formation, the remaining mutants showed WT–like dispersal, suggesting that canonical neurotransmission is unlikely to be the primary driver of this behavior (*SI Appendix*, Fig. S3 *A* and *B*). Given serotonin's conserved role in social behaviors across species (3, 40, 41, 45, 59) and its established function in modulating *C. elegans* foraging (46, 60, 61), we next focused on this pathway.

To examine whether serotonin contributes to swarming, we supplemented WT animals with exogenous serotonin. This treatment was sufficient to induce swarming (Fig. 3*A*), although the response was weaker than that seen in untreated *casy-1* mutants. In contrast, *casy-1* mutants were unaffected by serotonin (Fig. 3 *A* and *B*), suggesting that their serotonergic signaling might already be above baseline. To test whether this effect reflects a broader role of biogenic amines, we supplemented *C. elegans* with dopamine and octopamine. Despite evidence linking dopamine to social and aggregative behaviors (62, 63), neither WT nor *casy-1*

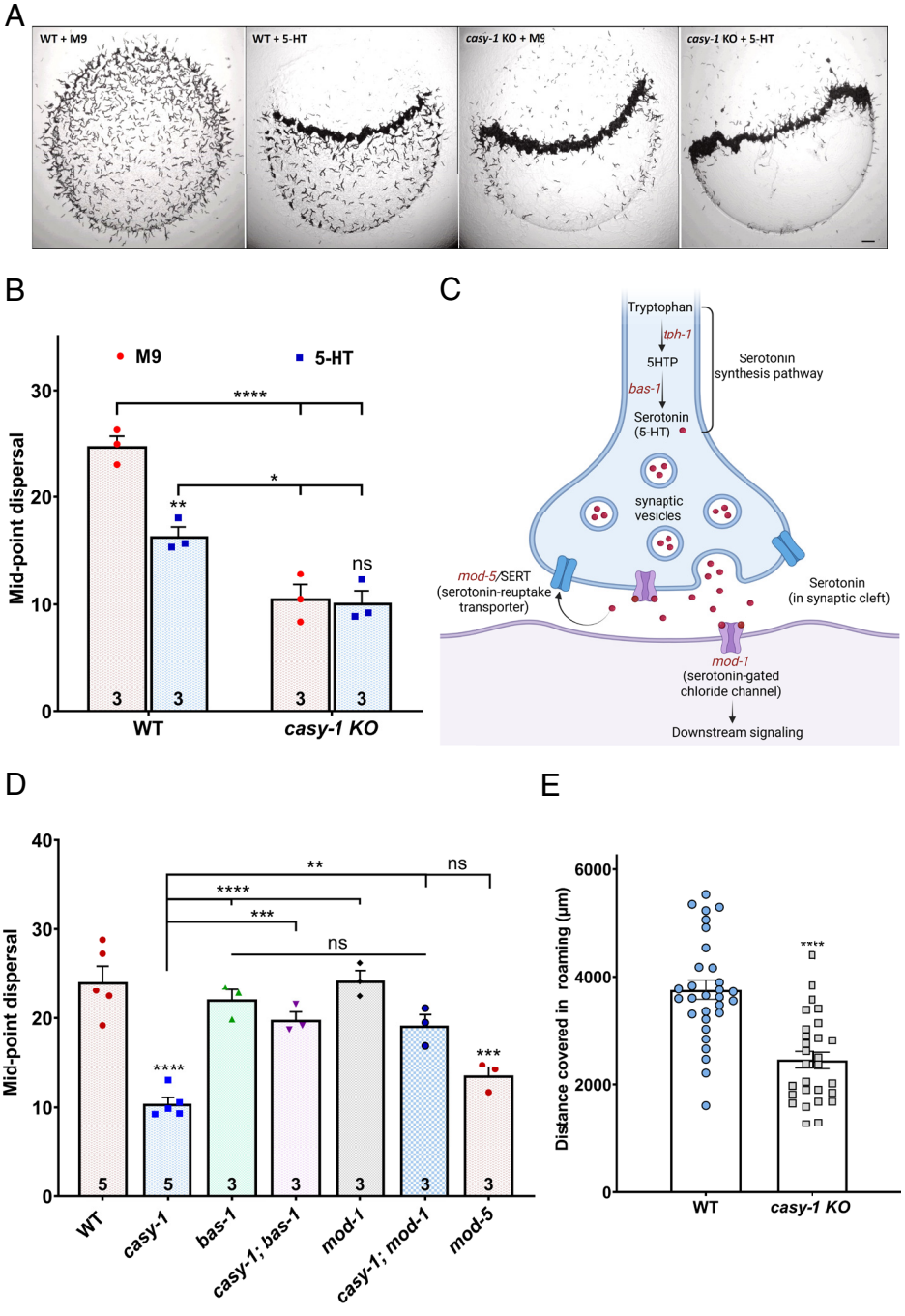

Fig. 3. Serotonin signaling contributes to swarming behavior in *casy-1* mutants. (*A*) Images showing the effect of serotonin (5-HT) supplementation on WT and *casy-1* mutant animals, with M9 buffer as a control. (Scale bar, 1 mm.) (*B*) Relative dispersal at the mid-point for WT and *casy-1* mutants supplemented with serotonin (5-HT, purple) or solvent control (M9, gray). WT animals show reduced dispersal with serotonin, while *casy-1* mutants exhibit no change. (*C*) Diagram of the serotonin signaling pathway. Tryptophan is converted to 5-HTP by *tph-1*, and then to serotonin by *bas-1*. Serotonin is packaged into vesicles, released into the synaptic cleft, and signals via *mod-1*, a serotonin-gated chloride channel. *mod-5* encodes the serotonin reuptake transporter (SERT). Image created with BioRender. (*D*) Mid-point dispersal for the indicated genotypes. Serotonin-deficient mutants (*bas-1*, *casy-1; bas-1*, *casy-1; mod-1*) resemble WT, while mutants with elevated serotonin signaling (*mod-1*, and *mod-5*) display reduced dispersal similar to *casy-1*. (*E*) Scatter plot showing total distance covered during roaming by individual WT and *casy-1* animals. *casy-1* mutants exhibit significantly reduced movement. Data are presented as mean ± SEM. For *B* and *D*, n = 3 biological replicates (plates) per group; replicate numbers are indicated within bars in panel *D*. For *E*, ~30 individual animals per genotype were analyzed. Statistical analysis was performed using one-way ANOVA with Tukey's post hoc test for *B* and *D* and unpaired *t* test with Welch's correction for *E*. Significance: (**P* < 0.05, ***P* < 0.01, *** < 0.001, *****P* < 0.0001; ns = nonsignificant). Representative videos corresponding to this figure are available in the OSF repository (54).

Downloaded from https://www.pnas.org by KOC UNIVERSITY LIBRARY on August 11, 2026 from IP address 88.255.99.16.

mutants showed any change in dispersal upon dopamine treatment (*SI Appendix*, Fig. S3 *C* and *D*). In contrast, prolonged exposure to octopamine significantly suppressed swarm formation in *casy-1* mutants, while producing no detectable effect in WT animals (*SI Appendix*, Fig. S3 *C* and *E*). This observation is consistent with previous reports showing that serotonin and octopamine act antagonistically to regulate food-dependent locomotion behaviors (64). Given that octopamine is also known to promote locomotion under fasting conditions (65), octopamine supplementation may artificially bias animals toward increased roaming, thereby suppressing swarm formation in *casy-1* mutants.

To further dissect serotonin's role, we examined its signaling pathway mutants (Fig. 3*C*). Mutants deficient in serotonin synthesis (*tph-1* and *bas-1*) showed WT dispersal (Fig. 3*D* and *SI Appendix*, Fig. S3*A*). We could not obtain double mutants of *casy-1* and *tph-1* as they are located close on the second chromosome. However, the *casy-1; bas-1* double mutants exhibited a strong suppression of the swarming observed in *casy-1* single mutants, reinforcing serotonin excess as a causal factor (Fig. 3*D*). We next examined *mod-1(ok103)* mutants, which lack the inhibitory serotonin-gated chloride channel. Consistent with previous reports (46, 60, 61), these mutants exhibited significantly increased dispersal compared to *casy-1* animals. We therefore analyzed *casy-1; mod-1* double mutants and found that loss of *mod-1* markedly suppressed swarm formation in *casy-1* mutants. In contrast, *mod-5* mutants, which accumulate extracellular serotonin due to defective reuptake, formed stable swarms similar to *casy-1* (Fig. 3*D*).

To further understand the behavioral effect of elevated serotonin, we quantified exploration in *casy-1* mutants. These animals showed significantly reduced exploratory behavior compared to WT (Fig. 3*E*). In *C. elegans*, serotonin typically promotes a shift from roaming to dwelling in response to food availability (46, 60, 61, 66). However, the clustering we observe in *casy-1* mutants differs from classic dwelling. These animals remain at the food boundary, rather than settling within the lawn, and show slowed locomotion even before food contact (*SI Appendix*, Fig. S2*A*). This suggests that the behavioral state is not triggered by food ingestion but instead reflects a serotonin-dependent internal state that mimics features of dwelling. Together, these findings support a model in which elevated serotonergic signaling contributes to the swarm formation in *casy-1* mutants.

PDF-1/PDFR-1 Signaling Functions Downstream of CASY-1 to Regulate Swarming. The behavioral features of *casy-1* mutants such as reduced exploration and slower locomotory speed (Fig. 3*E* and *SI Appendix*, Fig. S2*A*), resemble a dwelling-like state (46, 52). Since serotonin and Pigment dispersing factor 1 (PDF-1) function antagonistically to regulate dwelling and roaming in *C. elegans* (Fig. 4*A*), we investigated whether reduced PDF-1 signaling contributes to the swarming observed in *casy-1* mutants.

Mutants for *pdf-1*, *pdfr-1*, and *casy-1; pdf-1* double mutants showed persistent swarming, similar to *casy-1* alone (Fig. 4*B*). Expression of PDF-1 under its endogenous promoter rescued swarming in *pdf-1* mutants, confirming PDF-1's role. Interestingly, overexpression of PDF-1 in *casy-1* mutants suppressed swarming, suggesting that PDF-1 signaling is compromised in the absence of CASY-1 (Fig. 4*B*). To determine whether this reflects reduced expression of *pdf-1* or *pdfr-1* in *casy-1* mutants, we performed qPCR analysis and found no significant differences in transcript levels in *casy-1* mutants compared to WT (*SI Appendix*, Fig. S4*A*). We next examined the interdependence of serotonin and PDF-1 signaling in regulating swarming by analyzing *pdfr-1; mod-1* double mutants. These animals exhibited an intermediate phenotype, dispersing more than *casy-1* mutants yet forming swarm aggregates unlike WT animals (*SI Appendix*, Fig. S4*B*). This suggests that neither pathway is dominant; instead, serotonin and PDF-1 signaling act together in a dynamic balance.

To test circuit-level involvement, we optogenetically activated neurons expressing either PDF-1 or its receptor PDFR-1 (Fig. 4*C*). Blue-light stimulation of PDFR-1–expressing neurons robustly dispersed swarm aggregates in *casy-1* mutants, whereas activation of PDF-1–expressing neurons produced little to no effect (Fig. 4 *D* and *E*). One possible explanation for this could be that *casy-1* mutants have impaired PDF-1 trafficking, limiting its release and function despite optogenetic stimulation. Supporting this, CASY-1 and PDF-1 show overlapping expression in a subset of head sensory neurons (*SI Appendix*, Fig. S4*C*). In contrast, direct activation of PDFR-1–expressing neurons bypasses this defect and restores dispersal, suggesting that PDFR-1 neuron activity is sufficient to suppress swarming and acts downstream of *casy-1*. Control WT animals remained dispersed regardless of light exposure, and *casy-1* mutants lacking the transgene did not show light-induced changes in movement sufficient to disperse swarms, ruling out nonspecific light effects (Fig. 4*D*). Notably, optogenetic activation of CASY-1–expressing neurons also suppressed swarming, similar to PDFR-1 activation (Fig. 4*D*). Finally, to examine whether PDFR-1–expressing neuronal activation is sufficient to restore dispersal independently of ligand availability, we activated PDFR-1–expressing neurons in *pdf-1* and *pdfr-1* mutant backgrounds using the *Ppdfr-1::BlaC* transgene. In both cases, neuronal activation significantly increased dispersal, demonstrating that PDFR-1 activation alone is sufficient to overcome the behavioral defects associated with reduced PDF-1 signaling (Fig. 4*F*).

We also assessed whether this was a general defect in neuropeptide signaling. Both *egl-3* (neuropeptide processing) and *unc-31* (neuropeptide release) mutants, as well as their double mutants with *casy-1*, also showed swarming phenotypes (*SI Appendix*, Fig. S4*D*). A screen of other sensory-neuron-expressed neuropeptides and their receptors previously used to study foraging behaviors in our laboratory (67), revealed variable phenotypes (*SI Appendix*, Fig. S4*E*), indicating that diverse neuromodulatory pathways can influence swarming.

AIY-Dependent Locomotion Changes and Mechanosensory Outputs Downstream of PDFR-1 Signaling Contribute to Swarm Formation. Our results thus far indicate that reduced PDFR-1 signaling together with elevated serotonin signaling in *casy-1* mutants contributes to the swarming phenotype. This raises the question of where these pathways converge within the circuit and how their integration shapes behavior. AIY interneurons represent a plausible site of convergence, as they express both the serotonin-gated chloride channel MOD-1 and the PDFR-1 receptor (46) and function as a key interneuronal hub integrating multiple sensory inputs to regulate forward locomotion (68). Guided by prior work demonstrating that activity in a single interneuron can exert strong control over motor programs (69), we investigated the role of AIY interneurons in this context.

To examine the involvement of AIY in this circuit, we conditionally manipulated AIY interneuron activity using optogenetics. Optogenetic activation of AIY in *casy-1* mutants resulted in a significant increase in dispersal upon blue-light stimulation, whereas WT animals showed no detectable change in dispersal under the same conditions (Fig. 5*A* and *SI Appendix*, Fig. S5*A*). This indicates that AIY activation is sufficient to suppress swarming.

Conversely, optogenetic inactivation of AIY using the *AIY::Arch* line led to a pronounced reduction in locomotion and promoted swarm formation during red-light illumination (Fig. 5*B* and

Downloaded from https://www.pnas.org by KOC UNIVERSITY LIBRARY on August 11, 2026 from IP address 88.255.99.16.

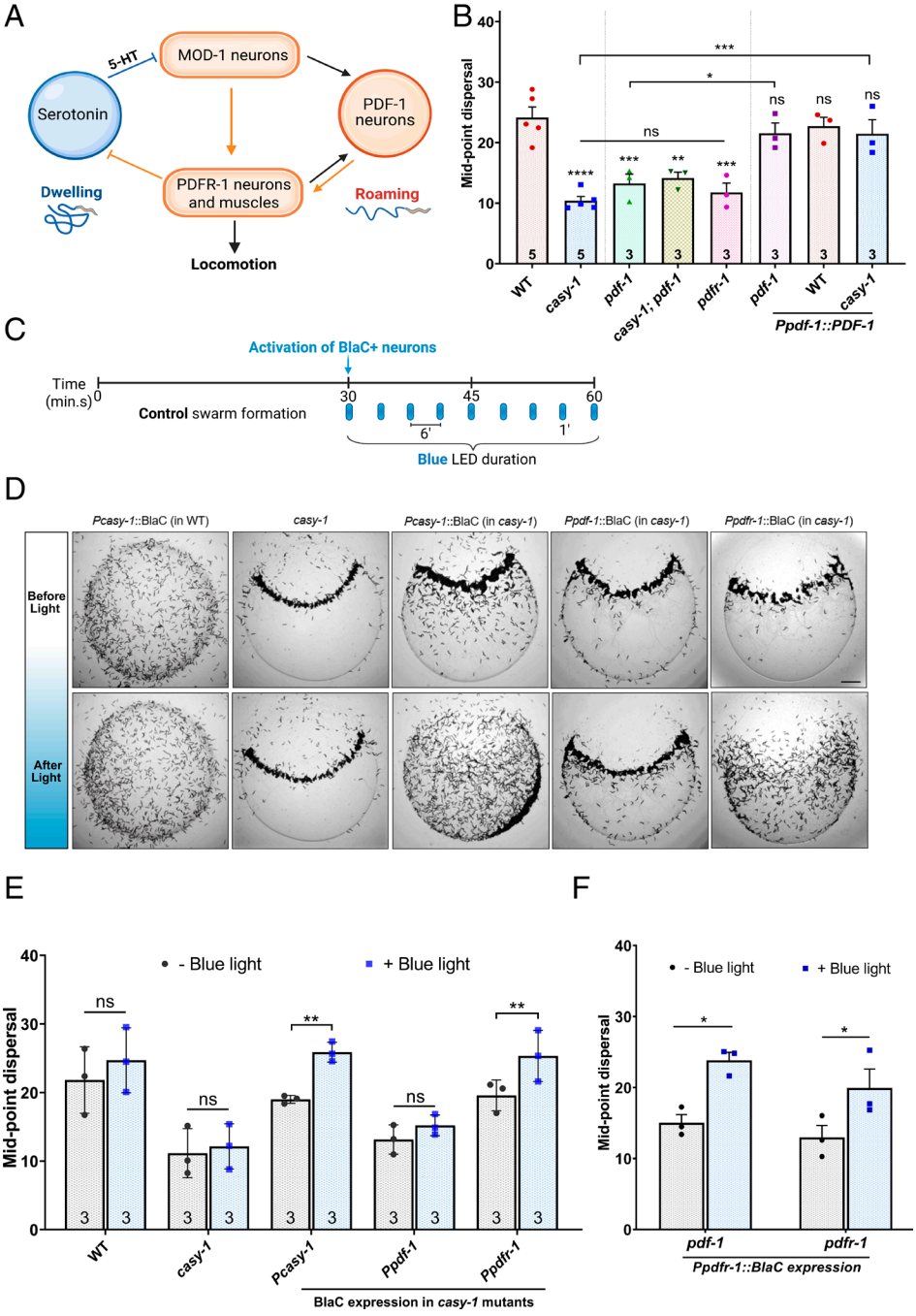

Fig. 4. CASY-1 regulates swarming through PDFR-1-dependent neuromodulatory signaling. (*A*) Schematic of the neuromodulatory circuit regulating behavioral state in *C. elegans*, illustrating antagonistic interactions between serotonin and PDF-1 pathways. Serotonin (5-HT), produced by NSM/HSN neurons (blue), promotes dwelling by inhibiting MOD-1–expressing neurons. PDF-1 (orange), released from AVB and PVP neurons acts via the receptor PDFR-1 to promote roaming. Adapted from ref. 61, created using BioRender. (*B*) Quantification of mid-point dispersal. *casy-1*, *pdf-1*, *casy-1; pdf-1*, and*pdfr-1* mutants all display swarm formation. Endogenous expression of *pdf-1* rescues dispersal in *pdf-1* mutants and *pdf-1* overexpression in *casy-1* mutants fully suppresses swarming. (*C*) Schematic showing the optogenetic stimulation paradigm using blue-light illumination (using Biorender). (*D*) Representative images showing *C. elegans* dispersal before and after blue light exposure in *Pcasy-1::BLaC* (WT), *casy-1* (no transgene), *Pcasy-1::BLaC* (*casy-1 KO*), *Ppdf-1::BLaC* (*casy-1* KO), and *Ppdfr-1::BLaC* (*casy-1 KO*) strains. (Scale bar, 1 mm.) (*E*) Quantification of dispersal before and after blue-light stimulation in strains expressing BLaC under different promoters. Blue light had no effect on WT controls (expressing *Pcasy-1::BLaC*) and *casy-1* mutants. In contrast, stimulation of *Pcasy-1*– or *Ppdfr-1*–driven BLaC in *casy-1* mutants significantly increased dispersal, while *Ppdf-1* activation showed no effect. (*F*) Activation of *Ppdfr-1::BLaC* restores dispersal in both *pdf-1* and *pdfr-1* mutant backgrounds, indicating that PDFR-1 neuronal activation is sufficient to bypass reduced PDF-1 signaling. Bar plots represent mean ± SEM. individual data points indicate biological replicates. Statistical tests: one-way ANOVA with Tukey's post hoc test; (* $P < 0.05$, *** $P < 0.001$, **** $P < 0.0001$; ns = nonsignificant). Representative videos corresponding to this figure are available in the OSF repository (54).

SI Appendix, Fig. S5*B*). Notably, precise temporal control of light exposure was required. Once a swarm consumed most of the food on the plate, animals often remained aggregated even after the light was turned off. We therefore turned off the light shortly (5 h) after initial swarm formation to assess whether this altered the behavioral outcome. These results demonstrate that AIY activity acts as a conditional switch to bias animals toward either dispersal or aggregation.

Importantly, the swarming induced by AIY inhibition is also evident at the level of individual *C. elegans* behavior. Single-worm trajectory analysis revealed that *Pttx-3::Arch* animals under illumination exhibit strong spatial confinement and local accumulation, closely resembling the restricted exploratory patterns observed in *casy-1* mutants (*SI Appendix*, Fig. S5*C* and Movies S5 and S6). While tracking animals over multiple days and analyzing their trajectories, we observed that WT animals dispersed their eggs broadly across the food lawn, whereas *casy-1* mutants laid eggs within more spatially confined regions (Movie S5). This localized egg deposition led to a local increase in population density in the subsequent generation, leading to swarm formation.

To confirm whether this phenotype arose from impaired dispersal rather than an overall increase in egg laying rate, we quantified egg-laying over a 6-d period. Although the total number of eggs laid by WT and *casy-1* mutants across this time window was comparable, *casy-1* mutants exhibited an earlier and sharper peak in egg-laying relative to WT animals (*SI Appendix*, Fig. S5*D*). These temporally clustered bouts of egg-laying in *casy-1* mutants may arise from their restricted locomotion and spatial confinement. However, we also speculate that elevated serotonin signaling in *casy-1* mutants could contribute to this altered egg-laying pattern. Such changes, in turn, reciprocally inhibit the PDFR-1 pathway and its downstream signaling.

Downloaded from https://www.pnas.org by KOC UNIVERSITY LIBRARY on August 11, 2026 from IP address 88.255.99.16.

Next, we examined how downstream signaling through PDFR-1 contributes to the swarming phenotype. PDFR-1 is expressed in mechanosensory neurons and muscles. It has been linked to touch- and mating-associated contact sensitivity (50, 52, 70). Based on this, we analyzed *mec-4* mutants, which are defective in gentle touch (71, 72), to assess whether mechanosensory input contributes to swarming; these mutants exhibited moderate swarming (Fig. 5*C*).

Mechanosensory feedback is known to affect collective behavior in *C. elegans* and other species (2, 73). To explore this, we measured head, anterior, and posterior touch responses in *casy-1*, *pdf-1*, and *pdfr-1* mutants, using *mec-4* as a control. *casy-1* mutants showed impaired responses to head and anterior touch. *pdfr-1* mutants showed reduced head sensitivity. *pdf-1* and WT animals responded normally. Posterior touch responses were intact in all genotypes (Fig. 5*D*).

These results suggest that *casy-1* mutants have reduced anterior mechanosensation. This may lower their ability to respond to nearby animals and help maintain clusters. We propose that impaired touch sensation, combined with neuromodulatory imbalance, lowered AIY neuron activity, supports the emergence and stability of swarms in *casy-1* mutants.

Mechanistic Model for CASY-1-Mediated Neuromodulatory Control of Swarming in *C. elegans*. Our data support a model in which loss of CASY-1 disrupts the balance between PDF-1/PDFR-1 and serotonin signaling, leading to altered behavioral state regulation and emergent swarming. In *casy-1* mutants, reduced PDFR-1 signaling together with elevated serotonin activity shifts animals toward a persistent dwelling-like state.

These two neuromodulatory pathways are known to mutually inhibit one another and converge on the AIY interneuron, a central hub for regulating transitions between roaming and dwelling. PDF-1 signaling promotes roaming via PDFR-1–expressing neurons, including AIY interneuron, whereas serotonin inhibits AIY activity through the MOD-1 receptor (46). Our finding that optogenetic silencing of AIY is sufficient to induce swarm formation in otherwise WT animals supports the role of AIY activity in controlling population dynamics.

CASY-1 is broadly expressed in sensory neurons and interneurons and partially overlaps with components of the PDF-1 and serotonin circuits, raising the possibility that it acts at multiple nodes within this network to maintain neuromodulatory balance (34, 74, 75). In *casy-1* mutants, this imbalance biases animals toward reduced roaming, slower locomotion, impaired mechanosensory responses, and increased dwelling.

Over time, these behavioral changes reduced dispersal, resulting in uncontrolled local increases in population density and ultimately swarm formation. We propose that this physical bottleneck provides the substrate for the spontaneous, self-organized emergence of swarming behavior observed in *casy-1* mutants (Fig. 6).

Discussion

Collective behaviors have been extensively examined through ethological and ecological lenses, offering key insights into the rules that guide group organization and dynamics (11, 77–79). However, the genetic and molecular mechanisms underlying these behaviors remain relatively unexplored. This gap may stem from the challenge of linking emergent population-level phenomena to specific molecular mechanisms. In this study, we leverage the genetic tractability of *C. elegans* to explore how a conserved synaptic protein, CASY-1, regulates a distinct swarming behavior via neuromodulatory signaling pathways.

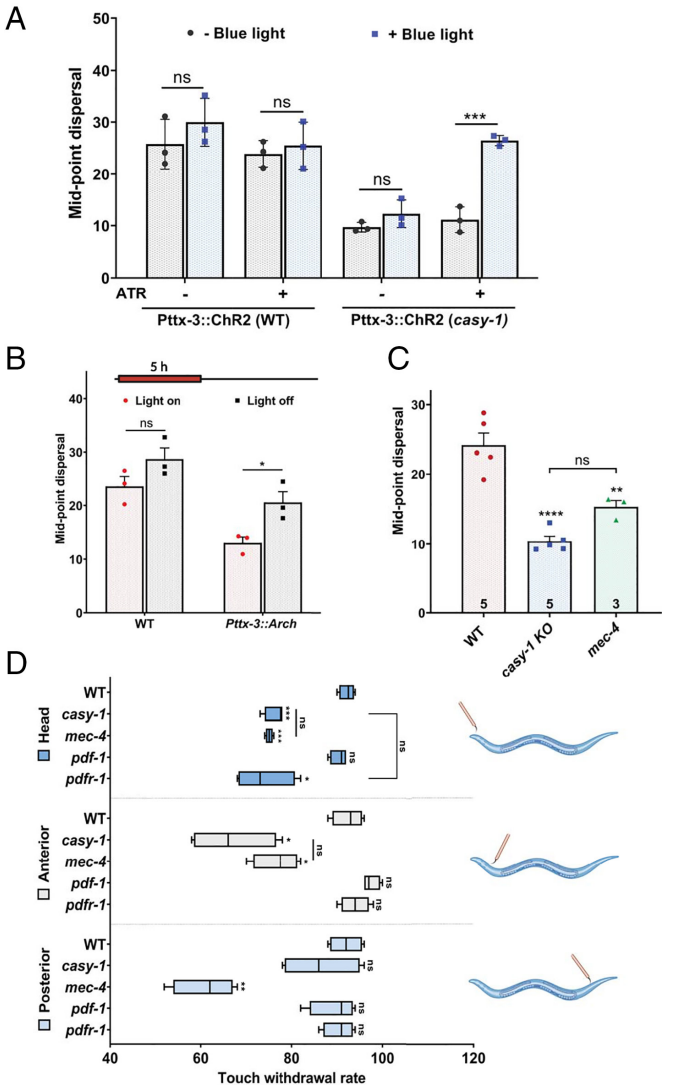

Fig. 5. AIY neuron activity regulates swarm formation and dispersal, modulated by mechanosensory inputs. (*A*) Optogenetic activation of AIY interneurons using *Pttx-3::Chr2* increases dispersal in *casy-1* mutants upon blue-light stimulation, whereas WT animals show no significant change. Animals tested in the presence (+ATR) or absence (−ATR) are indicated. (*B*) Optogenetic silencing of AIY using *Pttx-3::ArCh* promotes swarm formation. Mid-point dispersal decreases during red-light illumination (AIY silencing) and increases again after light withdrawal, indicating that reduced AIY activity results in aggregation. (*C*) Mid-point dispersal quantification in *casy-1* and *mec-4* mutants. *mec-4* animals, defective in gentle touch sensation, show reduced dispersal similar to *casy-1*. (*D*) Gentle touch responses scored as withdrawal rate (%) upon stimulation at head, anterior, and posterior body regions. *casy-1* and *pdfr-1* mutants show impaired head touch response, with *casy-1* also showing mild anterior defects. *mec-4* mutants serve as a negative control. Bar plots represent mean ± SEM, with individual data points indicating biological replicates. Statistical analyses were performed using one-way ANOVA with Tukey's post hoc test for dispersal assays (*A*–*C*) and two-way ANOVA with Tukey's post hoc test for touch-response assays (*D*). Touch assays are shown as box plots from four biological replicates (N = 10 *C. elegans* each). Significance is indicated as $*P < 0.05$, $***P < 0.001$, $****P < 0.0001$; ns = nonsignificant. Representative videos corresponding to this figure are available in the OSF repository (54).

We identify a self-organized, persistent swarming phenotype in *casy-1* mutants that emerges independently of the known environmental stressors. Unlike canonical aggregation responses triggered by hypoxia, starvation or crowding (16, 17, 20–22), swarming in *casy-1* mutants occurs even in nutrient-rich conditions (Fig. 1). This sustained clustering at the food boundary impairs optimal development, pointing to a potential ecological trade-off associated with prolonged group formation despite abundant resources. Notably,

Downloaded from https://www.pnas.org by KOC UNIVERSITY LIBRARY on August 11, 2026 from IP address 88.255.99.16.

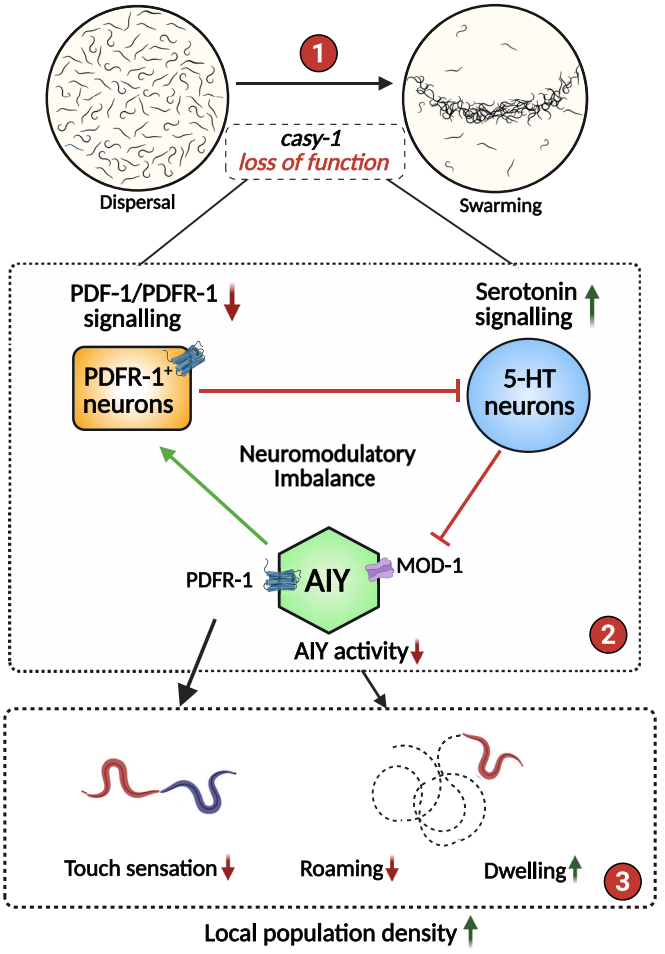

Fig. 6. Model for CASY-1–dependent neuromodulatory control of self-organized swarming behavior. The schematic illustrates the molecular, circuit-level, and behavioral changes describing how *casy-1* null mutation shifts animals from a dispersed state to a swarming state. (1) *casy-1* null mutation shifts animals from a dispersed state to a swarming state. (2) This transition is mediated by a neuromodulatory imbalance between the PDF-1/PDFR-1 pathway (↓) and the serotonergic system (↑). Reduced PDF-1 signaling fails to suppress serotonin activity, resulting in elevated serotonin levels, which inactivates AIY through the MOD-1 receptor resulting in decreased AIY activity. (3) The imbalance affects individual behavioral traits, including decreased speed, reduced roaming, increased dwelling, and impaired touch sensitivity, ultimately increasing the local population density. Arrows indicate activation (green), blunt lines indicate inhibition (red), and up/down arrows denote relative increases or decreases in activity or behavioral output. *C. elegans* trail is adapted from ref. 76, created using BioRender.

swarming appears to be self-reinforcing. For instance, once a small group began swarming, neighboring animals were more likely to join. However, we found no evidence for mediation by pheromones or extracellular vesicles (Fig. 2), suggesting the involvement of intrinsic pathways. Notably, a single *casy-1* mutant worm is sufficient to trigger swarm formation across generations, a phenomenon not observed in WT animals.

Our results reveal a conserved role for neuromodulatory balance in the emergence of swarming. We show that *casy-1* mutants have reduced Pigment-dispersing factor-1 (PDF-1) signaling, which correlates with elevated serotonin activity (Figs. 3–5). Serotonin is a conserved regulator of social behavior and has been implicated in disorders such as autism and depression (3, 40, 41, 45, 59). In *C. elegans*, serotonin promotes dwelling, while PDF-1 promotes roaming, and the two act antagonistically to regulate behavioral states (46). PDF-1 also tunes behavioral states in an evolutionary conserved manner, where in *Drosophila*, PDF controls circadian and arousal behaviors (80), and its mammalian homolog, vasoactive intestinal peptide (VIP), integrates neuromodulatory cues with circadian input to control arousal (81).

Calsyntenin orthologues are primarily characterized as postsynaptic signaling regulators, whereas CASY-1 functions mainly at the presynapse, influencing vesicular trafficking of neurotransmitters, localization of receptors, and CaMKII–MAPK pathway components (34, 35, 37, 58). It is known postsynaptic activity in *C. elegans* is limited to mediating AVG–HOA cell adhesion during development (82). A key mechanistic question is how CASY-1 functions within the swarming circuit. Our data indicate that its activity lies in sensory and interneurons, as CASY-1 expression under the motor neuron promoter (*Pcasy-1b*) does not rescue the phenotype (Fig. 1). Direct function at the motor neuron or muscle level therefore appears unlikely.

Our findings point to an indispensable role for the C-terminal domain in CASY-1 function. This domain has been implicated in vesicular trafficking through interactions with kinesin motors (34, 37, 58) and contains conserved Ca-binding sites that may influence vesicle release (83). These features raise the possibility that CASY-1 acts upstream as a vesicular cargo regulator. It may directly affect the transport or release of PDF-1– or PDFR-1–containing vesicles, or act indirectly through other mediators that reduce neuronal activity and thereby diminish PDF-1/PDFR-1 signaling. The absence of changes in *pdf-1* or *pdfr-1* transcript levels further support a posttranscriptional mode of regulation. Previous studies show that *casy-1* mutation increases glutamate release from sensory neurons, leading to elevated neuronal signaling (33). Such changes could enhance serotonin release, which in turn may reciprocally inhibit PDFR-1 activation (46). Given the broad expression of *casy-1* in several sensory and interneurons, it is conceivable that CASY-1 functions redundantly in this circuit (34, 74, 75). These possibilities remain to be tested to define the precise role of CASY-1 in modulating this neuromodulatory balance.

We show that *casy-1* mutants exhibit reduced PDFR-1 signaling. Optogenetic activation of PDFR-1 neurons and PDF-1 overexpression both induce dispersal in *casy-1* mutants, indicating reduced PDF-1 levels and a corresponding deficit in PDFR-1 pathway activation. Surprisingly, optogenetic activation of PDF-1 neurons does not suppress swarming, indicating that *casy-1* mutants may have impaired PDF-1 trafficking that limits its release and function despite neuronal stimulation. Overexpression likely bypasses this deficit by producing sufficient PDF-1 to overcome the release threshold.

PDFR-1 neuronal activation also rescues the phenotype in both *pdf-1* and *pdfr-1* mutants, indicating that the key regulatory step lies downstream of PDFR-1 activation. Activation of this pathway relieves inhibition of serotonin signaling, leading to elevated serotonin activity. This increase likely contributes to the localized egg-laying phenotype and reduced AIY activity, consistent with the presence of the serotonin-gated chloride channel MOD-1 in AIY. We show that AIY inhibition in WT animals induces swarm formation and localized movement even in single *C. elegans*, whereas AIY activation in *casy-1* mutants promotes dispersal by enhancing forward locomotion.

While our data support a model in which neuromodulatory imbalance drives swarming, some limitations remain. First, although grayscale-based analysis of population dispersal is useful for distinguishing between clearly swarming and nonswarming genotypes, it is less effective for mutants displaying intermediate or context-dependent behaviors. Quantitative metrics that better capture the degree and dynamics of aggregation will be useful. Second, we lack a clear understanding of how individual behavioral traits, such as movement characteristics, scale into group-level behavior. Although *casy-1* single mutants show reduced

Downloaded from https://www.pnas.org by KOC UNIVERSITY LIBRARY on August 11, 2026 from IP address 88.255.99.16.

locomotion speed and exploration (Figs. 2 and 3), their transition into clusters may also involve altered local interactions, possibly triggered by proximity to neighboring *C. elegans* in the swarm. Additionally, *casy-1* mutants exhibit impaired anterior mechanosensation, a phenotype also observed in *pdfr-1* mutants [Fig. 4, (70)]. Previous studies have shown that optogenetic activation of mechanosensory neurons can transiently disrupt *C. elegans* aggregates (73). Consistent with this, we found that *mec-4* mutants, which are defective in mechanosensation, also exhibit a tendency to form swarms. These observations suggest that reduced sensitivity to mechanical stimuli may help stabilize aggregates once they are formed. However, how these sensory changes integrate with neuromodulatory states to promote swarming remains unclear.

In summary, this study uncovers a role for CASY-1 in regulating swarming behavior through a conserved neuromodulatory pathway (Fig. 6). Future work combining circuit-level manipulations with theoretical behavioral modeling will be essential to dissect the neural mechanisms that shape group dynamics. Such insights could extend to broader contexts, including the neural basis of social behavior and its dysregulation in neurodevelopmental disorders.

Materials and Methods

***C. elegans* Strain Maintenance.** *C. elegans* strains were maintained on nematode growth medium (NGM) agar plates seeded with *Escherichia coli* OP50 at 22 °C, following standard protocols (84). The Bristol N2 strain served as the wild-type (WT) control. Stage-synchronized populations were obtained using sodium hypochlorite bleaching, as described previously (85). Unless otherwise specified, all experiments were conducted using young adult hermaphrodites. A complete list of strains used in this study is provided in *SI Appendix*, Table S2.

Generation of Constructs and Transgenic Lines. All plasmids were constructed either using Gibson assembly or restriction cloning and verified by sequencing prior to use. The transcriptional reporter *Pcasy-1::mCherry* was generated by promoter insertion upstream of mCherry in the pPD49.26 vector using restriction digestion. Rescue constructs for each *casy-1* isoform were generated by cloning the respective cDNA downstream of its promoter, with sequences obtained from WormBase as described previously (34). *BLaC* constructs were subcloned into the pSF154 Vector (46) by adding *Pcasy-1* and *Ppdf-1* promoter sequences. Transgenic *C. elegans* lines were generated by microinjection into the gonads of young adult hermaphrodites, using pCFJ90-mCherry or pCFJ90-GFP as coinjection markers as previously described (86). At least three independent lines were generated for each construct; the line with the highest expression penetrance and consistent behavior was selected for analysis. For all the rescue experiments, fluorescent transgenic *C. elegans* were enriched to approximately 80–90% of total population before starting the assay. Plasmids and transgenic strains used in this study are listed in *SI Appendix*, Tables S1 and S2, Primers in *SI Appendix*, Table S3.

CRISPR–Cas9 Genome Editing. CRISPR–Cas9 genome editing was performed following the protocol described in ref. 87. Full-gene and domain-specific knockouts of *casy-1* were generated in WT *C. elegans*. crRNAs were designed using the CRISPOR tool (88), selecting guides with high on-target scores and minimal off-target risk (*SI Appendix*, Table S3). crRNAs, tracrRNAs, and Cas9 protein were obtained from Integrated DNA Technologies (IDT). For N-terminal and C-terminal knockouts, a single-stranded DNA (ssDNA) repair template was also coinjected (*SI Appendix*, Table S3). The injection mix contained 0.25 μg/μL Cas9, 2.5 μM each of gRNA, and TE buffer (pH 7.5), incubated at 37 °C for 15 min. The coinjection marker pCFJ90 (5 ng/μL) was added, and the volume was adjusted to 20 μL with nuclease-free water. This mix was microinjected into young adult hermaphrodites. F1 animals expressing the pharyngeal marker were singled out and allowed to produce progeny. Genotyping of parent animals was performed using primers listed in *SI Appendix*, Figs. S1 and S2 and Table S3. Mutants carrying the desired deletion were homozygosed and outcrossed three times to WT to remove background mutations.

Swarming Behavior Recording. Approximately 700 to 800 synchronized young adult *C. elegans* were collected from 90 mm NGM plates using M9 buffer and washed to remove residual OP50 bacteria. The *C. elegans* were then transferred a few centimeters away from the food lawn on a 60 mm NGM plate seeded with 300 μL *E. coli* OP_{50} (OD = 2.5). As WT *C. elegans* also swarm at low food density, we selected a food OD threshold just above this range to ensure that swarming observed was specific to *casy-1* mutants. *C. elegans* behavior was recorded for 10 to 12 h at 22 °C under low-light conditions using the MBF Bioscience WormLab tracking system, until the food was used up. Experimenters were not blinded to genotype or condition, as swarming is a recorded, objectively quantified phenotype and does not involve subjective scoring.

Grayscale Quantification of Swarming. Swarming behavior was quantified using a grayscale intensity–based image analysis pipeline consisting of four steps: i) video preprocessing, ii) background subtraction, iii) binary segmentation, and iv) grayscale intensity measurement at defined equidistant time points. These measurements do not estimate absolute *C. elegans* population, but reliably capture the sharp contrast between the dense swarm core and the low-density peripheral regions. Because the *C. elegans* appear as dark objects against a lighter background, lower mean grayscale intensity corresponds to higher local animal density and vice-versa.

Raw video recordings were first time-lapsed (~512×) using OpenShot (v3.2.1), generating final clips of ~90 s. Videos were converted to .avi format using VLC Media Player (v3.0.21) for compatibility with Fiji (ImageJ v2.9.0). In Fiji, videos were opened as virtual stacks and converted to 8-bit grayscale images. A Z-projection of each stack was generated using the average intensity method and subtracted from the original stack using the "Image Calculator" function to remove static background features of the plate. Following background subtraction, binary images were generated to segment *C. elegans* clusters and eliminate frame-to-frame intensity variation unrelated to animal position. Binary masks were filtered using a uniform size threshold (2 to 4 pixels) to remove noise. From the processed stack, five frames evenly spaced across the total recording duration were selected, and mean grayscale intensity was measured over the defined lawn area for these frames.

To ensure consistent comparison across genotypes and experimental conditions and to avoid transient deviations at early or late stages of the assay, we defined a "mid-point dispersal" metric as the mean grayscale intensity measured at the temporal mid-point of each recording. This time point reproducibly corresponded to stabilized swarm organization across assays. Only the mid-point grayscale value was used for statistical analysis. For all displayed images and video frames, brightness and contrast were adjusted in PowerPoint to enhance visual clarity. These adjustments were applied uniformly across the entire image and did not affect data analysis, as quantification was performed on binary images independent of light intensity variations.

Single-Animal Foraging Assay. Foraging distance was measured on off-food 90 mm NGM plates lacking cholesterol. Plates were dried to remove excess moisture and equilibrated to room temperature (~22 °C) prior to use. Well-fed young adult *C. elegans* were gently transferred using an eyelash pick with a drop of halocarbon oil to an intermediate off-food plate to remove residual bacteria and then placed on the assay plate. The *C. elegans* were allowed to acclimate for 1 min before recording. Locomotion was recorded for 5 min using the MBF Bioscience WormLab imaging system at 8 fps. At least 20 *C. elegans* were recorded per genotype. Animals that moved out of the camera's field of view during the recording period were excluded from the analysis. Total distance (from the center-point) traveled per animal, as computed by WormLab software, was used as the primary readout and plotted using GraphPad Prism 9.5.1.

Aggregation Assay. Aggregation was assessed following established protocols (14, 15). Fresh 60 mm NGM plates were seeded with 200 μL of *E. coli* OP_{50} (OD_{600} ~1.5) to form a ~2.5 to 3 cm diameter circular lawn and dried to prevent the formation of a coffee ring. Approximately 70 synchronized young adult *C. elegans* were gently transferred to the center of the food lawn and allowed to settle for 1 h. Aggregation was manually scored thrice at 15-min intervals by counting the number of solitary, freely dispersing *C. elegans* and subtracting them from the total number of animals added on the plate. The remaining animals, found in groups near or at the food edge, were considered part of the aggregate. The assay was repeated three times per genotype across three independent days.

Single-Worm Temporal Tracking. Single-worm tracking was used to quantify long-term locomotion trajectories of individual animals. Young adult N2 and *casy-1 C. elegans* were tracked continuously for up to 3 d, until bacterial depletion

Downloaded from https://www.pnas.org by KOC UNIVERSITY LIBRARY on August 11, 2026 from IP address 88.255.99.16.

and crowding limited further recording. Imaging was performed at 5× magnification using a stereomicroscope equipped with motorized mechanical stages. Real-time image processing provided positional feedback to the motorized stage, enabling continuous centering of the animal within the field of view. Image frames and stage coordinates were recorded continuously for 3 d throughout the experiment, and full locomotion trajectories were reconstructed from the recorded data by using MATLAB-based custom code and visualized in Origin (2017).

Touch-Response Assay. Mechanosensory responses were assessed as previously described (89), using 60 mm NGM plates freshly seeded with OP_{50} (OD ~1.0). allowed to acclimate for 2 min before testing. All assays were performed blind to genotype. For the nose touch assay, each *C. elegans* was gently stimulated on the nose using an eyelash hair pick, ten times in succession, with a reversal movement scored as a positive response. For the anterior and posterior touch assays, animals were gently touched five times either just behind the pharynx (anterior) or near the tail (posterior). A reversal or forward movement, respectively, was counted as a positive response. Each assay was conducted in four independent replicates, with ten *C. elegans* per replicate. The total number of responses was recorded per animal, and results are reported as the mean percentage of positive responses per animal per genotype.

Serotonin Supplementation Assay. A 1 M serotonin hydrochloride stock solution (Sigma-Aldrich, SLCQ5039- H9523) was freshly prepared in sterile M9 buffer on the day of the experiment. Working concentrations of 3 mM, 6 mM, and 10 mM were tested based on prior studies (90), with 6 mM yielding the most consistent behavioral response. To ensure efficient uptake and minimize degradation during this longer, population-based assay (~500 *C. elegans* for this assay), animals were pre-exposed to serotonin (1,000 μL per 60 mm plate) in their synchronization plates for approximately 2.5 h before behavioral recording. In parallel, 60 mm NGM assay plates seeded with *E. coli* OP50 were evenly coated with 500 μL of the corresponding serotonin solution and dried in the dark. All plate preparations were conducted under low-light conditions to minimize photodegradation. *C. elegans* were then washed and transferred to one side of the assay plate, as described for swarming assays. Control plates were treated with sterile M9 buffer, and the animals were similarly exposed to buffer-only conditions to control for solvent effects. The data presented correspond to the 6 mM serotonin condition.

Optogenetics Assay. Optogenetic stimulation was performed using blue-light activation of adenylyl cyclase (BLaC), expressed under a cell-specific promoter as described previously (46). Transgenic *C. elegans* were generated by microinjecting the BLaC plasmid into the relevant mutant background, followed by crossing into WT to obtain a consistent genetic background. To prevent unintended activation, transgenic animals were maintained in light-protected containers wrapped in aluminum foil and handled under low-light conditions. Fluorescent animals were enriched before the assay by selecting for coinjection marker expression. For behavioral recordings, the transgenic animals were placed at one end of the bacterial lawn on a 60 mm plate and allowed to reach ~25% of the food lawn over 4 h in the dark. Behavior was then recorded for an hour using the MBF Bioscience WormLab tracking system. The first 30 min served as a baseline (no stimulation), followed by blue-light exposure during the next 30 min, delivered in 1-min pulses at six-min intervals (Fig. 4*C*). The plotted data represent the average grayscale intensity before and after stimulation, with the difference used to quantify the effect of neuronal activation on swarming behavior.

For channelrhodopsin-based optogenetic assays, a 100 mM stock solution of all-trans-retinal (ATR) was prepared in absolute ethanol. The stock was diluted to a final concentration of 100 μM in OP50, which was then seeded onto NGM plates and incubated overnight at room temperature. Plates were wrapped in aluminum foil throughout to minimize ATR oxidation and photodegradation. Because these experiments involved long-duration population assays, the remaining NGM surface of the 60-mm plates was additionally coated with 100 to 150 μL of 100 μM ATR and allowed to dry in the dark. Animals were then handled and assayed following the same paradigm described for the BlaC transgenic *C. elegans*.

For archaerhodopsin (Arch)-mediated optogenetic silencing, swarming behavior was recorded under continuous red LED illumination using the WormLab tracking system. Animals were exposed to red light for 5 h, after which the illumination was manually switched off while behavioral recording continued. For quantification, dispersal was measured using frames extracted at fixed time points (15 min before and 15 min after light offset). The difference in dispersal between these two time points was used to assess the effect of AIY silencing on swarm formation.

Statistical Analysis. All statistical analyses were performed using GraphPad Prism (9.5.1). The choice of statistical test and graph type depended on the data distribution and experimental design. Data were primarily represented using bar graphs and box-and-whisker plots. Comparisons between two groups were conducted using unpaired two-tailed Student's *t* tests with Welch's correction. For comparisons across more than two groups, one-way or two-way ANOVA followed by Tukey's multiple comparison test was applied. Time-course data were plotted as line graphs to visualize phenotypic changes over time. N refers to the number of technical replicates unless otherwise stated. Graphs display mean ± SEM, A P-value < 0.05 was considered statistically significant. For most figures, ($*P < 0.05$, $**P < 0.01$, $***P < 0.001$, $****P < 0.0001$; ns = not significant). Quantification was done using data from at least three independent biological replicates. The specific statistical test used for each dataset is detailed in the corresponding figure legend.

Data, Materials, and Software Availability. Representative videos, underlying datasets data have been deposited in Open Science Framework (https://osf.io/sxwjv/overview?view_only=423f3cb48e7541f997b08e21855b1194) (54). Other data are included in the article and/or supporting information.

ACKNOWLEDGMENTS. We thank Rohit Sachdeva and Kamal Kishore for invaluable contributions to video processing and quantification; Jagan J for help with CRISPR; Inchara M for experimental assistance; and Palagiri Suresh for his reliable routine support. We are deeply grateful to Hernán Jaramillo and Cori Bargmann for generously providing the PSF154 plasmid and MT9668 and CX14391 strains, Stephen Nurrish and Josh Kaplan for kindly sharing the KP1861 plasmid, and Kamal Kishore and Jagan J for the BAB8047 plasmid. We thank Isabel Beets, Arnab Mukhopadhyay, Umer Saleem, and Sharanya for generously sharing strains. We also thank Raghav Rajan, Arun SP, Anuradha Ratnaparkhi, and Arnab Barik for helpful suggestions. Some strains were obtained from the Caenorhabditis Genetics Center (CGC), supported by the NIH Office of Research Infrastructure Programs (P40 OD010440), and others from the National Bioresource Project (NBRP), Japan. We thank all members of the Kavita Babu lab for thoughtful feedback and critical reading of the manuscript, and we are grateful to the anonymous reviewers for their careful evaluation and suggestions. All illustrations were created with BioRender. The work was supported by an ANRF-POWER grant no. SPG/2022/000182 and a DBT/Wellcome Trust India Alliance Fellowship no. IA/S/19/2/504649. It was also part funded by a DBT Janaki Ammal National Women Bioscientist Award no. BT/HRD-NBA-NWB/38/2019-20 and ANRF Core Research grant no. CRG/2023/001950 awarded to K.B. NS was supported by a CSIR-NET fellowship. The funders had no role in experimental design, data collection or analysis, decision to publish, or preparation of the manuscript.

Author affiliations: [a]Centre for Neuroscience, Indian Institute of Science, Bangalore, Karnataka 560012, India; [b]Department of Biological Sciences, Indian Institute of Science Education and Research, Berhampur 760010, India; [c]School of Bio Sciences and Technology, Vellore Institute of Technology, Vellore 632014, India; and [d]Department of Physics, Koç University, Istanbul 34450, Türkiye

Author contributions: N.S., A.K., and K.B. designed research; N.S., N.K., S.K., D.D., E.S., and A.K. performed research; N.S. contributed new reagents/analytic tools; N.S., N.K., and A.K. analyzed data; K.B. supervisory role, helped with writing and editing the manuscript, received funding for the research; and N.S. wrote the paper.

1. I. D. Couzin, Collective animal migration. *Curr. Biol.* **28**, R976–R980 (2018).
2. P. Ramdya *et al.*, Mechanosensory interactions drive collective behaviour in *Drosophila*. *Nature* **519**, 233–236 (2015).
3. M. L. Anstey, S. M. Rogers, S. R. Ott, M. Burrows, S. J. Simpson, Serotonin mediates behavioral gregarization underlying swarm formation in desert locusts. *Science* **323**, 627–630 (2009).
4. A. Selimbeyoglu *et al.*, Modulation of prefrontal cortex excitation/inhibition balance rescues social behavior in CNTNAP2-deficient mice. *Sci. Transl. Med.* **9**, eaah6733 (2017).
5. C. S. Muirhead, J. Srinivasan, Small molecule signals mediate social behaviors in C. elegans. *J. Neurogenet.* **34**, 395–403 (2020).
6. R. Harpaz *et al.*, Collective behavior emerges from genetically controlled simple behavioral motifs in zebrafish. *Sci. Adv.* **7**, eabi7460 (2021).

Downloaded from https://www.pnas.org by KOC UNIVERSITY LIBRARY on August 11, 2026 from IP address 88.255.99.16.

7. M. H. Cowen *et al.*, Conserved autism-associated genes tune social feeding behavior in *C. elegans*. *Nat. Commun.* **15**, 9301 (2024).
8. I. Janczarek, A. Wisniewska, M. H. Chruszczewski, E. Tkaczyk, A. Gorecka-Bruzda, Social behaviour of horses in response to vocalisations of predators. *Animals (Basel)* **10**, 2331 (2020).
9. F. Hiramatsu, J. W. Lightfoot, Kin-recognition and predation shape collective behaviors in the cannibalistic nematode *Pristionchus pacificus*. *PLoS Genet.* **19**, e1011056 (2023).
10. M. J. Hansen, P. Domenici, P. Bartashevich, A. Burns, J. Krause, Mechanisms of group-hunting in vertebrates. *Biol. Rev. Camb. Philos. Soc.* **98**, 1687–1711 (2023).
11. D. J. Sumpter, The principles of collective animal behaviour. *Philos. Trans. R. Soc. Lond. B. Biol. Sci.* **361**, 5–22 (2006).
12. M. C. Leung *et al.*, *Caenorhabditis elegans*: An emerging model in biomedical and environmental toxicology. *Toxicol. Sci.* **106**, 5–28 (2008).
13. H. Jang *et al.*, Dissection of neuronal gap junction circuits that regulate social behavior in *Caenorhabditis elegans*. *Proc. Natl. Acad. Sci. U.S.A.* **114**, E1263–E1272 (2017).
14. M. de Bono, C. I. Bargmann, Natural variation in a neuropeptide Y receptor homolog modifies social behavior and food response in *C. elegans*. *Cell* **94**, 679–689 (1998).
15. E. Z. Macosko *et al.*, A hub-and-spoke circuit drives pheromone attraction and social behaviour in *C. elegans*. *Nature* **458**, 1171–1175 (2009).
16. S. S. Ding, L. S. Muhle, A. E. X. Brown, L. J. Schumacher, R. G. Endres, Comparison of solitary and collective foraging strategies of *Caenorhabditis elegans* in patchy food distributions. *Philos. Trans. R. Soc. Lond. B. Biol. Sci.* **375**, 20190382 (2020).
17. S. S. Ding, L. J. Schumacher, A. E. Javer, R. G. Endres, A. E. Brown, Shared behavioral mechanisms underlie *C. elegans* aggregation and swarming. *Elife* **8**, e43318 (2019).
18. M. de Bono, D. M. Tobin, M. W. Davis, L. Avery, C. I. Bargmann, Social feeding in *Caenorhabditis elegans* is induced by neurons that detect aversive stimuli. *Nature* **419**, 899–903 (2002).
19. N. Zjacic, M. Scholz, The role of food odor in invertebrate foraging. *Genes Brain Behav.* **21**, e12793 (2022).
20. B. H. Cheung, M. Cohen, C. Rogers, O. Albayram, M. de Bono, Experience-dependent modulation of C. elegans behavior by ambient oxygen. *Curr. Biol.* **15**, 905–917 (2005).
21. J. M. Gray *et al.*, Oxygen sensation and social feeding mediated by a C. elegans guanylate cyclase homologue. *Nature* **430**, 317–322 (2004).
22. E. Demir, Y. I. Yaman, M. Basaran, A. Kocabas, Dynamics of pattern formation and emergence of swarming in *Caenorhabditis elegans*. *Elife* **9**, e52781 (2020).
23. K. C. Reddy, R. C. Hunter, N. Bhatla, D. K. Newman, D. H. Kim, *Caenorhabditis elegans* NPR-1-mediated behaviors are suppressed in the presence of mucoid bacteria. *Proc. Natl. Acad. Sci. U.S.A.* **108**, 12887–12892 (2011).
24. T. Elmer, C. Stadtfeld, Depressive symptoms are associated with social isolation in face-to-face interaction networks. *Sci. Rep.* **10**, 1444 (2020).
25. C. A. Depp *et al.*, Social competence and observer-rated social functioning in bipolar disorder. *Bipolar Disord.* **12**, 843–850 (2010).
26. M. C. Roozen, M. J. H. Kas, Assessing genetic conservation of human sociability-linked genes in *C. elegans*. *Behav. Genet.* **55**, 141–152 (2025).
27. D. D. Ikeda *et al.*, CASY-1, an ortholog of calsyntenins/alcadeins, is essential for learning in Caenorhabditis elegans. *Proc. Natl. Acad. Sci. U.S.A.* **105**, 5260–5265 (2008).
28. C. Preuschhof *et al.*, KIBRA and CLSTN2 polymorphisms exert interactive effects on human episodic memory. *Neuropsychologia* **48**, 402–408 (2010).
29. A. Vagnoni *et al.*, Calsyntenin-1 mediates axonal transport of the amyloid precursor protein and regulates Abeta production. *Hum. Mol. Genet.* **21**, 2845–2854 (2012).
30. S. V. Ranneva, K. S. Pavlov, A. V. Gromova, T. G. Amstislavskaya, T. V. Lipina, Features of emotional and social behavioral phenotypes of calsyntenin2 knockout mice. *Behav. Brain Res.* **332**, 343–354 (2017).
31. K. Mori *et al.*, Loss of calsyntenin paralogs disrupts interneuron stability and mouse behavior. *Mol. Brain* **15**, 23 (2022).
32. T. V. Lipina *et al.*, Cognitive deficits in calsyntenin-2-deficient mice associated with reduced GABAergic transmission. *Neuropsychopharmacology* **41**, 802–810 (2016).
33. S. Thapliyal, S. Ravindranath, K. Babu, Regulation of glutamate signaling in the sensorimotor circuit by CASY-1A/calsyntenin in *Caenorhabditis elegans*. *Genetics* **208**, 1553–1564 (2018).
34. S. Thapliyal *et al.*, The C-terminal of CASY-1/Calsyntenin regulates GABAergic synaptic transmission at the Caenorhabditis elegans neuromuscular junction. *PLoS Genet.* **14**, e1007263 (2018).
35. N. Shahi, S. Thapliyal, K. Babu, Sensory modulation of neuropeptide signaling by CASY-1 gates cholinergic transmission at Caenorhabditis elegans neuromuscular junction. *J. Biosci.* **50** (2025).
36. F. J. Hoerndli *et al.*, A conserved function of C. elegans CASY-1 calsyntenin in associative learning. *PLoS One* **4**, e4880 (2009).
37. H. Ohno *et al.*, Role of synaptic phosphatidylinositol 3-kinase in a behavioral learning response in *C. elegans*. *Science* **345**, 313–317 (2014).
38. J. C. Coates, M. de Bono, Antagonistic pathways in neurons exposed to body fluid regulate social feeding in *Caenorhabditis elegans*. *Nature* **419**, 925–929 (2002).
39. C. Rogers *et al.*, Inhibition of *Caenorhabditis elegans* social feeding by FMRFamide-related peptide activation of NPR-1. *Nat. Neurosci.* **6**, 1178–1185 (2003).
40. D. Kiser, B. Steemers, I. Branchi, J. R. Homberg, The reciprocal interaction between serotonin and social behaviour. *Neurosci. Biobehav. Rev.* **36**, 786–798 (2012).
41. J. Bacque-Cazenave *et al.*, Serotonin in animal cognition and behavior. *Int. J. Mol. Sci.* **21**, 1649 (2020).
42. J. F. Kamhi, S. Arganda, C. S. Moreau, J. F. A. Traniello, Origins of aminergic regulation of behavior in complex insect social systems. *Front. Syst. Neurosci.* **11**, 74 (2017).
43. P. M. Whitaker-Azmitia, Behavioral and cellular consequences of increasing serotonergic activity during brain development: A role in autism? *Int. J. Dev. Neurosci.* **23**, 75–83 (2005).
44. D. I. Zafeiriou, A. Ververi, E. Vargiami, The serotonergic system: Its role in pathogenesis and early developmental treatment of autism. *Curr. Neuropharmacol.* **7**, 150–157 (2009).
45. J. Golebiowska *et al.*, Serotonin transporter deficiency alters socioemotional ultrasonic communication in rats. *Sci. Rep.* **9**, 20283 (2019).
46. S. W. Flavell *et al.*, Serotonin and the neuropeptide PDF initiate and extend opposing behavioral states in *C. elegans*. *Cell* **154**, 1023–1035 (2013).
47. N. Pokala, E. E. Glater, Using optogenetics to understand neuronal mechanisms underlying behavior in *C. elegans*. *J. Undergrad. Neurosci. Educ.* **16**, A152–A158 (2018).
48. J. Watteyne, A. Chudinova, L. Ripoll-Sanchez, W. R. Schafer, I. Beets, Neuropeptide signaling network of *Caenorhabditis elegans*: From structure to behavior. *Genetics* **228**, iyae141 (2024).
49. D. Chen, K. P. Taylor, Q. Hall, J. M. Kaplan, The neuropeptides FLP-2 and PDF-1 act in concert to arouse Caenorhabditis elegans locomotion. *Genetics* **204**, 1151–1159 (2016).
50. A. Barrios, R. Ghosh, C. Fang, S. W. Emmons, M. M. Barr, PDF-1 neuropeptide signaling modulates a neural circuit for mate-searching behavior in *C. elegans*. *Nat. Neurosci.* **15**, 1675–1682 (2012).
51. J. Luo, D. S. Portman, Sex-specific, pdfr-1-dependent modulation of pheromone avoidance by food abundance enables flexibility in *C. elegans* foraging behavior. *Curr. Biol.* **31**, 4449–4461.e4 (2021).
52. T. Janssen *et al.*, Functional characterization of three G protein-coupled receptors for pigment dispersing factors in *Caenorhabditis elegans*. *J. Biol. Chem.* **283**, 15241–15249 (2008).
53. M. Toth, The other side of the coin: Hypersociability. *Genes Brain Behav.* **18**, e12512 (2019).
54. N. Shahi, K. Babu, Data from "Neuromodulation of swarming behavior in *Caenorhabditis elegans*: Insights into the conserved role of calsyntenins." Open Science Framework. https://osf.io/sxwjv/overview?view_only=423f3cb48e7541f997b08e21855b1194. Deposited 15 December 2025.
55. S. Thapliyal, K. Babu, Pentylenetetrazole (PTZ)-induced convulsion assay to determine GABAergic defects in Caenorhabditis elegans. *Bio. Protoc.* **8**, e2989 (2018).
56. B. H. Cheung, F. Arellano-Carbajal, I. Rybicki, M. de Bono, Soluble guanylate cyclases act in neurons exposed to the body fluid to promote *C. elegans* aggregation behavior. *Curr. Biol.* **14**, 1105–1111 (2004).
57. J. Wang *et al.*, Ciliary intrinsic mechanisms regulate dynamic ciliary extracellular vesicle release from sensory neurons. *Curr. Biol.* **34**, 2756–2763.e2 (2024).
58. C. Ding, Y. Wu, H. Dabas, M. Hammarlund, Activation of the CaMKII-Sarm1-ASK1-p38 MAP kinase pathway protects against axon degeneration caused by loss of mitochondria. *Elife* **11**, e73557 (2022).
59. D. S. Dwyer, Crossing the worm-brain barrier by using *Caenorhabditis elegans* to explore fundamentals of human psychiatric illness. *Mol. Neuropsychiatry* **3**, 170–179 (2018).
60. U. Dag *et al.*, Dissecting the functional organization of the C. elegans serotonergic system at whole-brain scale. *Cell* **186**, 2574–2592.e20 (2023).
61. N. Ji *et al.*, A neural circuit for flexible control of persistent behavioral states. *Elife* **10**, e62889 (2021).
62. B. Chen *et al.*, Sulfation modification of dopamine in brain regulates aggregative behavior of animals. *Natl. Sci. Rev.* **9**, nwab163 (2022).
63. D. S. Dwyer, P. Awatramani, R. Thakur, R. Seeni, E. J. Aamodt, Social feeding in *Caenorhabditis elegans* is modulated by antipsychotic drugs and calmodulin and may serve as a protophenotype for asociality. *Neuropharmacology* **92**, 56–62 (2015).
64. M. A. Churgin, R. J. McCloskey, E. Peters, C. Fang-Yen, Antagonistic serotonergic and octopaminergic neural circuits mediate food-dependent locomotory behavior in Caenorhabditis elegans. *J. Neurosci.* **37**, 7811–7823 (2017).
65. J. He, G. Ou, W. Li, Fasting rescues locomotion in neuromodulation-deficient C. elegans via octopamine–Gαq signaling. *Biol. Cell* **117**, e70043 (2025).
66. J. Ben. Arous, S. Laffont, D. Chatenay, Molecular and sensory basis of a food related two-state behavior in C. elegans. *PLoS One* **4**, e7584 (2009).
67. U. S. Bhat *et al.*, FLP-15 functions through the GPCR NPR-3 to regulate local and global search behaviours in Caenorhabditis elegans. bioRxiv [Preprint] (2025). https://doi.org/10.1101/2025.05.02.651881 (Accessed 24 June 2025).
68. J. M. Gray, J. J. Hill, C. I. Bargmann, A circuit for navigation in *Caenorhabditis elegans*. *Proc. Natl. Acad. Sci. U.S.A.* **102**, 3184–3191 (2005).
69. A. Kocabas, C. H. Shen, Z. V. Guo, S. Ramanathan, Controlling interneuron activity in *Caenorhabditis elegans* to evoke chemotactic behaviour. *Nature* **490**, 273–277 (2012).
70. S. Choi, M. Chatzigeorgiou, K. P. Taylor, W. R. Schafer, J. M. Kaplan, Analysis of NPR-1 reveals a circuit mechanism for behavioral quiescence in *C. elegans*. *Neuron* **78**, 869–880 (2013).
71. K. Hong, M. Driscoll, A transmembrane domain of the putative channel subunit MEC-4 influences mechanotransduction and neurodegeneration in C. elegans. *Nature* **367**, 470–473 (1994).
72. H. Suzuki *et al.*, In vivo imaging of C. elegans mechanosensory neurons demonstrates a specific role for the MEC-4 channel in the process of gentle touch sensation. *Neuron* **39**, 1005–1017 (2003).
73. T. Sugi, H. Ito, M. Nishimura, K. H. Nagai, C. Elegans collectively forms dynamical networks. *Nat. Commun.* **10**, 683 (2019).
74. A. Ghaddar *et al.*, Whole-body gene expression atlas of an adult metazoan. *Sci. Adv.* **9**, eadg0506 (2023).
75. M. Majeed, C. P. Liao, O. Hobert, Nervous system-wide analysis of all C. elegans cadherins reveals neuron-specific functions across multiple anatomical scales. *Sci. Adv.* **11**, eads2852 (2025).
76. V. Padmanabhan *et al.*, Locomotion of *C. elegans*: A piecewise-harmonic curvature representation of nematode behavior. *PLoS One* **7**, e40121 (2012).
77. C. Heins *et al.*, Collective behavior from surprise minimization. *Proc. Natl. Acad. Sci. U.S.A.* **121**, e2320239121 (2024).
78. D. M. Perez *et al.*, Towering behavior and collective dispersal in *Caenorhabditis* nematodes. *Curr. Biol.* **35**, 2980–2986.e4 (2025).
79. C. N. Cook *et al.*, Individual learning phenotypes drive collective behavior. *Proc. Natl. Acad. Sci. U.S.A.* **117**, 17949–17956 (2020).
80. A. Sehgal, E. Mignot, Genetics of sleep and sleep disorders. *Cell* **146**, 194–207 (2011).
81. A. M. Vosko, A. Schroeder, D. H. Loh, C. S. Colwell, Vasoactive intestinal peptide and the mammalian circadian system. *Gen. Comp. Endocrinol.* **152**, 165–175 (2007).
82. B. Kim, S. W. Emmons, Multiple conserved cell adhesion protein interactions mediate neural wiring of a sensory circuit in *C. elegans*. *Elife* **6**, e29257 (2017).
83. L. Vogt *et al.*, Calsyntenin-1, a proteolytically processed postsynaptic membrane protein with a cytoplasmic calcium-binding domain. *Mol. Cell. Neurosci.* **17**, 151–166 (2001).
84. S. Brenner, The genetics of *Caenorhabditis elegans*. *Genetics* **77**, 71–94 (1974).
85. M. Porta-de-la-Riva, L. Fontrodona, A. Villanueva, J. Ceron, Basic Caenorhabditis elegans methods: Synchronization and observation. *J. Vis. Exp.* **10**, e4019 (2012).
86. C. Mello, A. Fire, DNA transformation. *Methods Cell Biol.* **48**, 451–482 (1995).
87. K. S. Ghanta, T. Ishidate, C. C. Mello, Microinjection for precision genome editing in *Caenorhabditis elegans*. *STAR Protoc.* **2**, 100748 (2021).
88. J. P. Concordet, M. Haeussler, CRISPOR: Intuitive guide selection for CRISPR/Cas9 genome editing experiments and screens. *Nucleic Acids Res.* **46**, W242–W245 (2018).
89. M. Chalfie *et al.*, The neural circuit for touch sensitivity in *Caenorhabditis elegans*. *J. Neurosci.* **5**, 956–964 (1985).
90. E. K. C. Schwartz *et al.*, Serotonin and dopamine mimic glucose-induced reinforcement in *C. elegans*: Potential role of NSM neurons and the serotonin subtype 4 receptor. *Front. Physiol.* **12**, 783359 (2021).

Downloaded from https://www.pnas.org by KOC UNIVERSITY LIBRARY on August 11, 2026 from IP address 88.255.99.16.